

# Synthesis of RCCC Linkages to Visit Four Given Poses

Shaoping Bai<sup>1</sup>

Department of Mechanical and  
Manufacturing Engineering,  
Aalborg University,  
Denmark  
e-mail: shb@m-tech.aau.dk

Jorge Angeles

Department of Mechanical Engineering,  
McGill University,  
Montreal, Canada  
e-mail: angeles@cim.mcgill.ca

*This paper focuses on the problem of synthesis of spatial four-bar linkages of the RCCC type for rigid-body guidance with four given poses,  $R$  denoting a revolute,  $C$  a cylindrical kinematic pair. While synthesis equations for  $CC$  and  $RC$  dyads are available in the literature, the synthesis of spatial RCCC four-bar linkages requires special attention, due to its asymmetric topology. We revisit the problem to cope robustly with the asymmetry, namely, the approximate nature of the  $RC$  dyad and the infinity of exact solutions of the  $CC$  dyad for the number of given poses. Our approach includes a robust formulation of the synthesis of  $CC$  dyads, for the determination of axis-congruences. Moreover, we formulate a uniform synthesis equation, which enables us to treat both  $RC$  and  $CC$  dyads, with properly selected constraints for both cases. Two design examples are included. [DOI: 10.1115/1.4028637]*

## 1 Introduction

The *Burmester problem* is concerned with finding the geometric parameters of a four-bar linkage whose coupler link is to visit a given set of finitely separated poses. The problem is also known as linkage synthesis for *rigid-body guidance* or, equivalently, for *motion generation*.

The Burmester problem has been studied for planar, spherical, and spatial linkages. Compared with the extensive studies on the planar and spherical Burmester problems, that associated with the synthesis of spatial linkages for rigid-body guidance, however, has received much less attention. A relative paucity of works is known on the synthesis of spatial four-bar linkages [1–10]. Of these works, Larochelle [6] studied the synthesis of  $CC$  dyads—a dyad is nothing but a *binary* link carrying one kinematic pair at each of its extremities—for four poses. Wampler et al. [7] developed a *continuation* method that, when applied to the synthesis of spatial mechanisms, leads to all possible solutions, real and complex. Murray and McCarthy [8] investigated the determination of central-axis congruences associated with the synthesis of spatial  $CC$  dyads.

In the spatial rigid-body guidance problem, the synthesis of spatial RCCC four-bar linkages requires special attention, due to its asymmetric topology. A RCCC linkage can be produced upon assembling one  $RC$  dyad with one  $CC$  dyad, each with its own set of constraints. The difference is apparent in both the number and the type of constraints. For this reason, solutions to  $CC$  and  $RC$  dyads have to be found separately for the same set of given poses. For  $CC$ -dyads, exact solutions can be found with five given poses (including the reference pose). On the other hand, a  $RC$ -dyad does not admit exact solutions for four given poses [3,11].

This paper focuses on the problem of synthesis of spatial four-bar linkages of the RCCC type for rigid-body guidance through four given poses. While synthesis equations were formulated by Tsai and Roth [3] for  $CC$  and  $RC$  dyads, we revisit the problem regarding the *approximate* synthesis of the  $RC$  dyad, while coping with the infinity of  $CC$ -dyads within a novel approach. This includes a robust formulation of the synthesis of  $CC$  dyads for the determination of axis-congruences. Moreover, we formulate the  $RC$  dyad synthesis with properly selected constraints to guarantee the generation of a  $RC$  dyad. Design examples are included.

The formulation of synthesis equations in this work is developed by extending the authors' previous work [10], in which dual algebra was adopted at the level of problem formulation. Dual algebra exploits the *Principle of Transference* [12] to derive the synthesis equations for spatial linkages using those of their spherical counterparts. In this formulation, we address not only the geometric relationships between the design task and the possible linkages but also the formulation robustness.

## 2 Problem Formulation

A generic spatial four-bar linkage of the RCCC type is depicted in Fig. 1. As the coupler link 3 moves, while visiting  $m$  given poses besides the reference pose, the moving axes  $Z_3$  and  $Z_4$ , represented by the dual unit vectors  $\hat{a}_0$  and  $\hat{a}_0^*$  at the reference pose, attain  $m$  locations. A line being defined by a point and a direction, the line is short of one dimension<sup>2</sup> to occupy a rigid-body pose. Henceforth, a *line location* will be understood as given by four independent parameters, grouped in a six-dimensional array of Plücker coordinates [13]. The location of a rigid body, known as

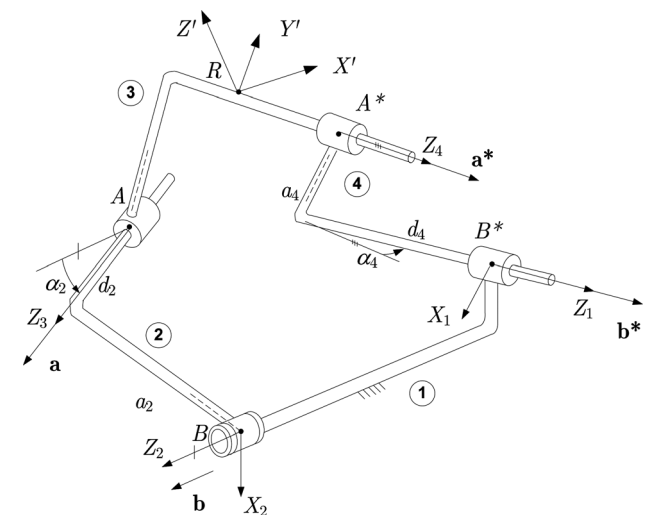


Fig. 1 The RCCC linkage, where all four links are indexed with numbers

<sup>1</sup>Corresponding author.

Contributed by the Mechanisms and Robotics Committee of ASME for publication in the JOURNAL OF MECHANISMS AND ROBOTICS. Manuscript received June 21, 2013; final manuscript received September 10, 2014; published online December 4, 2014. Assoc. Editor: Qiaode Jeffrey Ge.

<sup>2</sup>Upon adding one dimension to a line, namely, a point outside of the line, a plane is obtained, which is capable of attaining a full pose.

the body *pose*, is defined by six independent parameters. A displacement undergone by a line is also known as an *incompletely specified rigid-body displacement* [14]. The  $m$  locations of the  $Z_3$ -axis are represented by the dual unit vectors  $\hat{\mathbf{a}}_1, \dots, \hat{\mathbf{a}}_m$ , those of the  $Z_4$ -axis by  $\hat{\mathbf{a}}_1^*, \dots, \hat{\mathbf{a}}_m^*$ .

Likewise, the dual unit vectors of the fixed axes  $Z_1$  and  $Z_2$  are represented by the dual unit vectors  $\hat{\mathbf{b}}$  and  $\hat{\mathbf{b}}^*$ , respectively. With the foregoing framework, the spatial Burmester problem is stated as:

Find a spatial RCCC linkage that will conduct its coupler link through a set  $S$  of  $m$  poses, given by the orthogonal matrices  $\{\mathbf{Q}_j\}_1^m$  and points  $\{\mathbf{R}_j\}_1^m$  of the coupler link, of position vectors  $\{\mathbf{r}_j\}_1^m$ , defined with respect to a reference pose, given by  $\mathbf{Q}_0 = \mathbf{I}$  and  $\mathbf{r}_0 = \mathbf{0}$ .

In the above statement,  $\mathbf{I}$  denotes the  $3 \times 3$  identity matrix and  $\mathbf{0}$  the three-dimensional zero vector. Moreover, the body under guidance is rigidly attached to link 3, and hence, the body poses are referred to the frame with origin at  $R_0$ , the reference position of point  $R$  of Fig. 1, and axes  $X_0, Y_0, Z_0$ , shown unsubscripted at the arbitrary pose of link 3 in the foregoing figure. Furthermore, in the problem at hand,  $m = 3$ .

### 3 Synthesis of CC and RC Dyads

The synthesis of the RCCC linkage is based on that of the four-bar spherical linkage, shown in Fig. 2.

For quick reference, the synthesis of the spherical linkage is briefly recalled. The main issue in this problem is the location of the fixed axes  $\overline{OB}$  and  $\overline{OB}^*$  as well as those of their moving counterparts,  $\overline{OA}$  and  $\overline{OA}^*$ , at the *reference pose* of the coupler link. Within the approach adopted at the outset, one RR dyad  $\overline{AB}$  is now synthesized. As the synthesis problem associated with this dyad admits up to six solutions [11], the maximum number of linkage solutions is 15, the number of combinations of six objects taking two at a time.

Furthermore, the synthesis equations of the RR dyad of interest rely on the constancy of angle  $\alpha_2$  throughout the various locations adopted by lines  $\mathcal{A}$  and  $\mathcal{B}$  as the coupler link visits the  $m$  given poses, which in this case reduce to attitudes. Let  $\mathbf{a}_0$  denote the (unit) position vector of  $A_0$ , i.e., the position of  $A$  at the reference attitude of the coupler link,  $\mathbf{a}_j$  denoting the (unit) position vector of the same point at the  $j$ th attitude of the same link. Constancy of  $\alpha_2$  throughout the  $m$  attitudes thus requires

$$\mathbf{a}_j^T \mathbf{b} = \mathbf{a}_0^T \mathbf{b} \equiv \cos \alpha_2, \quad j = 1, \dots, m \quad (1a)$$

with  $\mathbf{b}$  denoting the (unit) position vector of  $B$ , and  $\mathbf{a}_j$  obtained as the image of  $\mathbf{a}_0$  under a rotation represented by matrix  $\mathbf{Q}_j$ :

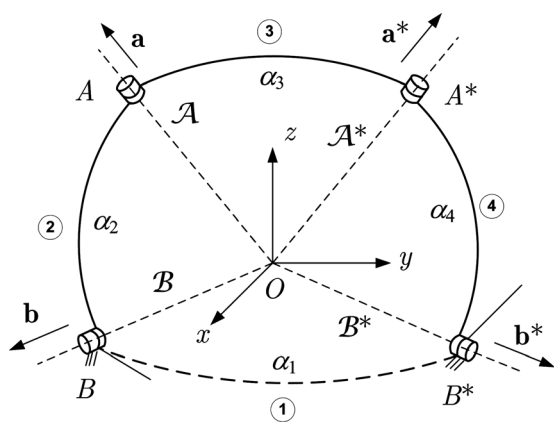


Fig. 2 The spherical 4R linkage, where all four bodies are indexed with numbers

$$\mathbf{a}_j = \mathbf{Q}_j \mathbf{a}_0, \quad j = 1, \dots, m \quad (1b)$$

We undertake now the synthesis of the CC and RC dyads. With reference to the spatial linkage of Fig. 1, joint axes  $Z_3$  and  $Z_4$ , which define uniquely the coupler link, undergo a spatial motion while visiting the  $m$  given poses. The spatial displacement of the moving axis  $Z_3$  in terms of dual vectors can be described by mimicking Eq. (1b), if with the real quantities of this equation replaced with dual quantities, namely,

$$\hat{\mathbf{a}}_j = \hat{\mathbf{Q}}_j \hat{\mathbf{a}}_0, \quad j = 1, \dots, m \quad (2)$$

where  $\hat{\mathbf{a}}_0$  is the dual representation of line  $Z_3$  at the reference pose of the coupler link, while  $\hat{\mathbf{Q}}_j$  is the *dual orthogonal matrix* representing the spatial displacement of the coupler link, namely,

$$\hat{\mathbf{a}}_0 = \mathbf{a}_0 + \varepsilon \bar{\mathbf{a}}_0, \quad \hat{\mathbf{Q}}_j = \mathbf{Q}_j + \varepsilon \bar{\mathbf{Q}}_j \quad (3)$$

where  $\varepsilon$  is the dual unity, which verifies  $\varepsilon \neq 0, \varepsilon^2 = 0$ , and  $\mathbf{a}_0$  denotes the unit vector parallel to  $Z_3$  at its reference pose, while  $\bar{\mathbf{a}}_0$  the *moment* of the same axis with respect to the origin  $R_0$  of the frame  $\{X_0, Y_0, Z_0\}$ , with subscript 0 denoting the *reference pose* of the frame attached to link 3 in Fig. 1. Moreover,  $\mathbf{Q}_j$  is the proper orthogonal matrix that rotates the coupler link from its 0th to its  $j$ th attitude. In addition,  $\bar{\mathbf{Q}}_j$  is the product of a *translation matrix*  $\mathbf{R}_j$  by  $\mathbf{Q}_j$ , i.e.,

$$\bar{\mathbf{Q}}_j = \mathbf{R}_j \mathbf{Q}_j \quad (4)$$

with  $\mathbf{R}_j$  defined as the *cross-product matrix* of vector  $\mathbf{r}_j$ , i.e.,  $\mathbf{R}_j \equiv \text{CPM}(\mathbf{r}_j) \equiv \partial(\mathbf{r}_j \times \mathbf{v}) / \partial(\mathbf{v}), \forall \mathbf{v} \in \mathbb{R}^3$ , for a translation  $\mathbf{r}_j$  of point  $R$  at the  $j$ th pose of link 3.

As the *relative location* of  $Z_3$  with respect to  $Z_2$  remains constant throughout the motion of the coupler link, the dual angle between the two axes remains constant, and hence,

$$\hat{\mathbf{a}}_j^T \hat{\mathbf{b}} = \cos(\alpha_2 + \varepsilon \alpha_2) \equiv \cos \alpha_2 - \varepsilon \alpha_2 \sin \alpha_2, \quad j = 0, \dots, m \quad (5)$$

where  $\hat{\mathbf{b}}$  is the dual unit vector representing the  $Z_2$  axis, which includes point  $B$ , is given by

$$\hat{\mathbf{b}} = \mathbf{b} + \varepsilon \bar{\mathbf{b}} \quad (6)$$

with  $\alpha_2, \alpha_2$ , and  $\mathbf{b}$  shown in Fig. 1, while vector  $\bar{\mathbf{b}}$  denotes the moment of  $Z_2$  with respect to  $R_0$ . Subtracting the 0th equation from its  $m$  remaining counterparts, Eq. (5) leads to

$$(\hat{\mathbf{a}}_j - \hat{\mathbf{a}}_0)^T \hat{\mathbf{b}} = 0, \quad j = 1, \dots, m \quad (7)$$

In the sequel, a single notation for the  $m+1$  location of the  $Z_3$ -axis will be needed. To avoid double subscripts,  $Z_3$  will be labeled line  $\mathcal{A}$ . Now, the geometric interpretation of Eq. (7) is that, as line  $\mathcal{A}$  adopts the set of locations  $\{\mathcal{A}_j\}_1^m$ , it remains equidistant from  $Z_2$ , which means that line  $\mathcal{A}_j$  remains at the same Euclidian distance from and making the same angle with  $Z_2$ . As a consequence, Eq. (7) constrains line  $\mathcal{A}$  to be a line of the same regulus of a single-fold hyperboloid of revolution of axis  $Z_2$ .

Equation (7), upon expansion into its primal and dual parts, for  $j = 1, \dots, m$ , yields two systems of real scalar equations

$$\mathbf{a}_0^T (\mathbf{Q}_j^T - \mathbf{1}) \mathbf{b} = 0 \quad (8a)$$

$$\mathbf{a}_0^T \bar{\mathbf{Q}}_j^T \mathbf{b} + \mathbf{a}_0^T (\mathbf{Q}_j^T - \mathbf{1}) \bar{\mathbf{b}} + \bar{\mathbf{a}}_0^T (\mathbf{Q}_j^T - \mathbf{1}) \mathbf{b} = 0 \quad (8b)$$

whose unknowns,  $\mathbf{a}_0, \bar{\mathbf{a}}_0, \mathbf{b}$ , and  $\bar{\mathbf{b}}$ , are subject to the constraints

$$\mathbf{a}_0^T \bar{\mathbf{a}}_0 = 0, \quad \mathbf{b}^T \bar{\mathbf{b}} = 0 \quad (9a)$$

$$\|\mathbf{a}_0\|^2 = 1, \quad \|\mathbf{b}\|^2 = 1 \quad (9b)$$

We thus have  $m$  real equations (8a) for the primal and  $m$  real equations (8b) for the dual part. Of these, Eq. (8a) involves only unit vectors of the joint axes, while Eq. (8b) involves both unit and moment vectors. Therefore, while the left-hand side of Eq. (8a) is dimensionless that of Eq. (8b) has units of length. The first set is called the *direction*, the second the *moment equations* [11]. Both sets stand for the basic geometric constraints on different dyads, including CC, RC, and RR. Furthermore, Equations (8a) are exactly the synthesis equations for the spherical four-bar linkage, illustrated in Fig. 2, under motion generation.<sup>3</sup>

The direction equations (8a) are independent of the moment equations (8b), which means that the unit vectors  $\mathbf{a}_0$  and  $\mathbf{b}$  are determined by direction equations alone, if these involve as many equations as unknowns. This is the case of synthesis for five prescribed poses. On the other hand, the moment equations include the unit vectors  $\mathbf{a}_0$  and  $\mathbf{b}$ . Moreover, these equations are linear in the dual parts, which means that, upon solving for the unit vectors, the dual parts can be obtained from linear equations.

**3.1 The CC Dyad.** The CC dyad under synthesis consists of one rigid link and two C joints. The dyad can be geometrically regarded as a link composed of two skew lines, joined to each other by means of a third line, their common normal, for example. A CC dyad is thus determined once the two skew lines are known. The problem of CC-dyad synthesis thus reduces to locating the two joint axes. The latter can be uniquely described by means of the dual vectors  $\hat{\mathbf{a}}_0$  and  $\hat{\mathbf{b}}$ , which comprise a total of 12 scalar components. Note that  $\mathbf{a}_0$  and  $\mathbf{b}$  are unit vectors, while a line can be regarded as a zero-pitch screw [11], as expressed by Eqs. (9a) and (9b). Those four scalar constraints thus reduce the number of independent variables to only eight.

Equations (8a) and (8b) lead to  $2m$  synthesis equations for  $m$  given poses. For the number of given poses to yield as many equations as unknowns, i.e., eight, one must have  $2m = 8$ . The system thus admits exact solutions for CC dyads in the case of  $m = 4$ , i.e., for five given poses, a well-known result.

Knowing that the direction equations are independent of the moment equations, we can find first the direction vectors  $\mathbf{a}_0$  and  $\mathbf{b}$  through Eqs. (8a). These equations, identical to those of the Burmester problem for spherical linkages, admit at most six real solutions. With each such solution, the moment equations become linear in the moments, namely,

$$\mathbf{p}_j^T \bar{\mathbf{a}}_0 + \mathbf{q}_j^T \bar{\mathbf{b}} = w_j, \quad j = 1, \dots, m \quad (10)$$

with

$$\mathbf{p}_j = (\mathbf{Q}_j^T - \mathbf{1})\mathbf{b}, \quad \mathbf{q}_j = (\mathbf{Q}_j - \mathbf{1})\mathbf{a}_0, \quad w_j = -\bar{\mathbf{a}}_0^T \bar{\mathbf{Q}}_j^T \bar{\mathbf{b}} \quad (11)$$

Equations (9a) and (10) amount to six linear equations for six unknowns in the case of  $m = 4$ , thus defining a unique pair of moments,  $\bar{\mathbf{a}}_0$  and  $\bar{\mathbf{b}}$ , in the absence of singularities.

The six linear equations mentioned above can be cast in vector form, namely,

$$\mathbf{M}\mathbf{x} = \mathbf{n} \quad (12)$$

<sup>3</sup>That is, if abstraction is made of the translation of the coupler link when formulating the problem stated in Section 2, then points  $R_j$ , for  $j = 1, \dots, m$ , coincide with point  $R_0$ , and the problem at hand becomes one of spherical-linkage synthesis.

where

$$\mathbf{M} = \begin{bmatrix} \mathbf{p}_1^T & \mathbf{q}_1^T \\ \mathbf{p}_2^T & \mathbf{q}_2^T \\ \mathbf{p}_3^T & \mathbf{q}_3^T \\ \mathbf{p}_4^T & \mathbf{q}_4^T \\ \mathbf{a}_0^T & \mathbf{0}^T \\ \mathbf{0}^T & \mathbf{b}^T \end{bmatrix}, \quad \mathbf{x} = \begin{bmatrix} \bar{\mathbf{a}}_0 \\ \bar{\mathbf{b}} \end{bmatrix}, \quad \mathbf{n} = \begin{bmatrix} w_1 \\ w_2 \\ w_3 \\ w_4 \\ 0 \\ 0 \end{bmatrix} \quad (13)$$

with  $\mathbf{0}$  denoting the three-dimensional zero vector; hence,  $\mathbf{M}$  is apparently a  $6 \times 6$  matrix.

Equation (12) admits unique solutions for five given poses ( $m = 4$ ). With four poses given ( $m = 3$ ), a total of five equations are obtained from Eqs. (8a) and (8b). In this case, the system of synthesis equations is underdetermined, and, hence, infinitely many solutions are possible. These solutions can be regarded as sets of lines, called *congruences*, which define the moving and fixed axes. The generation of line congruences is described in Sec. 4.

**3.2 The RC Dyad.** A RC dyad is composed of a revolute and a cylindrical joint. The synthesis equations for the CC spatial dyad also apply to the RC dyad. Moreover, compared with the CC dyad, the RC dyad is subject to one constraint: the sliding  $s_j$  along the fixed axis, shown in Fig. 3, is zero. This constraint can be expressed in terms of the dual vector of the common normal.

For the  $j$ th pose, the common normal to  $\mathcal{A}_j$  and  $Z_2$  is given by the normalized—i.e., of dual unit norm—vector  $\hat{\mathbf{n}}_j \times \hat{\mathbf{b}}$ , denoted by  $\hat{\mathbf{n}}_j$ , namely [10]

$$\hat{\mathbf{n}}_j = \mathbf{n}_j + \varepsilon \bar{\mathbf{n}}_j, \quad j = 0, \dots, m \quad (14)$$

with

$$\mathbf{n}_j = \frac{1}{\sin \alpha_2} (\mathbf{a} \times \mathbf{b}), \quad \bar{\mathbf{n}}_j = \frac{1}{\sin \alpha_2} (\mathbf{a}_j \times \bar{\mathbf{b}} + \bar{\mathbf{a}}_j \times \mathbf{b}) - \frac{a_2 \cos \alpha_2}{\sin^2 \alpha_2} (\mathbf{a}_j \times \mathbf{b}) \quad (15)$$

where  $a_2$  and  $\alpha_2$  are the distance and the angle between  $\mathcal{A}_j$  and  $Z_2$ , respectively. The dual angle between two poses of the common normals,  $\hat{\mathbf{n}}_j$  and  $\hat{\mathbf{n}}_0$ , can be found from

$$\cos \hat{\beta}_j = \hat{\mathbf{n}}_j^T \hat{\mathbf{n}}_0, \quad j = 1, \dots, m \quad (16)$$

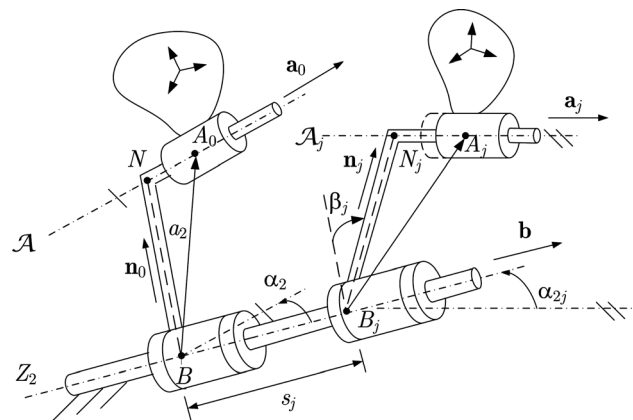


Fig. 3 A CC dyad, which becomes a RC dyad if the sliding  $s_j$  vanishes

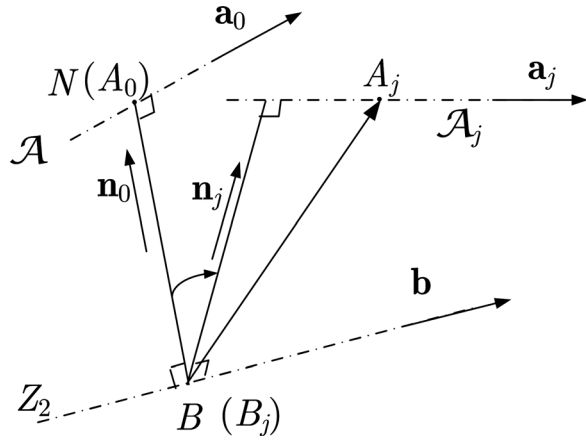


Fig. 4 Geometric relations in the RC dyad

where  $\hat{\beta}_j = \beta_j + \varepsilon s_j$ , with  $\beta_j$  and  $s_j$  denoting the  $j$ th rotation and the  $j$ th sliding of the  $R$  joint of Fig. 3, respectively. Equating the dual parts of the expanded equation (16) leads to

$$-s_j \sin \beta_j = \frac{1}{\sin^3 \alpha_2} (A_j a_2 \cos \alpha_2 - B_j \sin \alpha_2) \quad (17)$$

with

$$A_j = 2(\mathbf{a}_0 \times \mathbf{b})^T (\mathbf{a}_j \times \mathbf{b}) \quad (18)$$

$$B_j = (\mathbf{a}_0 \times \mathbf{b})^T (\mathbf{a}_j \times \bar{\mathbf{b}} + \bar{\mathbf{a}}_j \times \mathbf{b}) + (\mathbf{a}_j \times \mathbf{b})^T (\mathbf{a}_0 \times \bar{\mathbf{b}} + \bar{\mathbf{a}}_0 \times \mathbf{b}) \quad (19)$$

For RC dyads,  $s_j = 0$ , while, for spatial dyads,  $\sin \alpha_2$  does not vanish,<sup>4</sup> and, hence, Eq. (17) yields

$$A_j a_2 \cos \alpha_2 - B_j \sin \alpha_2 = 0, \quad j = 1, \dots, m \quad (20)$$

which is the set of constraint equations needed to guarantee the vanishing of the sliding on the fixed axis.

**An Alternative Formulation:** Equation (20) leads to a lengthy expression, as seen from Eqs. (18) and (19), while  $a_2$  and  $\alpha_2$  are design variables. A simpler expression of the constraint can be derived from the geometric relationship between three vectors, namely, the common normal vector and the two unit vectors parallel to lines  $\mathcal{A}_j$  and  $Z_2$ . With reference to Fig. 3, where  $B_j$  and  $N_j$  are the intersections of the common normal  $\mathcal{N}_j$  with lines  $Z_2$  and  $\mathcal{A}_j$ , point  $A_0$  being located on the coupler link and lying in line  $\mathcal{A}_j$ .

Because of the constraint on the  $R$  joint,  $B_j$  remains at the same location as  $B$ . Henceforth,  $B_j$  is thus replaced by  $B$ . Three vectors, namely,  $\mathbf{a}_j$ ,  $\mathbf{n}_j$ , and  $\mathbf{r}_{A_j} - \mathbf{r}_B$ , for  $j = 1, \dots, m$ , must remain coplanar for all configurations, as illustrated in Fig. 4. This constraint is expressed as

$$\mathbf{a}_j \times \mathbf{n}_j \cdot (\mathbf{r}_{A_j} - \mathbf{r}_B) = 0, \quad j = 1, \dots, m \quad (21)$$

where  $\mathbf{r}_{A_j} = \mathbf{r}_j + \mathbf{Q}_j \mathbf{r}_{A_0}$  and  $\mathbf{n}_j = \mathbf{a}_j \times \mathbf{b}$ . In this formulation, the unknowns are  $\mathbf{r}_B$  and  $\mathbf{r}_{A_0}$ , in addition to  $\mathbf{b}$  and  $\mathbf{a}$ .

The initial configuration, for  $j = 0$ , defines where the two points  $A_0$  and  $B$  are located. As  $A_0B$  is a segment of the common normal to the lines  $Z_2$  and  $\mathcal{A}_j$ , the conditions below have to be met

$$\mathbf{a}_0 \cdot (\mathbf{r}_{A_0} - \mathbf{r}_B) = 0; \quad \mathbf{b} \cdot (\mathbf{r}_{A_0} - \mathbf{r}_B) = 0 \quad (22)$$

Apparently, the foregoing moment equations bear units of length. To make the solution scale-independent, it is advisable to normalize the lengths, which can be achieved by making use of a *characteristic length*, denoted as  $\lambda$ . Equations (21) and (22) can be normalized with the characteristic length, to be defined in Sec. 3.2.1, as

$$\mathbf{a}_j \times \mathbf{n}_j \cdot \mathbf{d}_j = 0, \quad j = 1, \dots, m \quad (23)$$

$$\mathbf{a}_0 \cdot \mathbf{d}_0 = 0, \quad \mathbf{b} \cdot \mathbf{d}_0 = 0 \quad (24)$$

where  $\mathbf{d}_j = (\mathbf{r}_{A_j} - \mathbf{r}_B)/\lambda$ ,  $j = 0, \dots, m$ . Equations (23) and (24) represent the geometric constraints for a RC dyad on the vanishing of the  $R$  joint sliding.

**3.2.1 Equation Normalization.** In following common engineering practice, the moment equations are henceforth normalized, upon dividing them by the *characteristic length*  $\lambda$  obtained from the problem data and introduced in Eq. (23).

It is known that, to any rigid body motion, a displacement screw is associated, which is determined by a line  $\mathcal{L}$ , the screw axis, and a pitch  $p$ . It is known, moreover, that the displacement of any point on the body has the same projection onto the axis of rotation [15]. For the displacement from the reference pose to the  $j$ th pose, this projection,  $d_j$ , is given by

$$d_j = \mathbf{e}_j \cdot \mathbf{r}_j, \quad j = 1, \dots, m \quad (25)$$

where  $\mathbf{e}_j$  is the unit vector parallel to the axis of rotation and  $\mathbf{r}_j$  the displacement of point  $R$  of the coupler link. Noting that the displacement involves a rotation  $\psi_j$ , the “pitch” of the associated displacement screw is thus<sup>5</sup>

$$p_j = d_j/\psi_j \quad (26)$$

The characteristic length is defined as [17]

$$\lambda = \max_j \{|p_j|\}_1^m \quad (27)$$

The equation involving the moments  $\bar{\mathbf{a}}_j$  and  $\bar{\mathbf{b}}$  is now normalized upon dividing the vectors by  $\lambda$ , which thus leads to the nondimensional variables

$$\mathbf{u}_j = \frac{1}{\lambda} \bar{\mathbf{a}}_j, \quad \mathbf{v} = \frac{1}{\lambda} \bar{\mathbf{b}} \quad (28)$$

**3.3 Approximate Solution of the RC-Dyad Synthesis.** For a RC spatial dyad, we have so far formulated constraint equations (8a), (8b), (23), and (24), which amount to  $3m$  equations for  $m$  poses. Note that the problem bears eight independent unknowns, which means that, for a RC-dyad synthesis problem to lead to as many equations as unknowns,  $m$  must be  $8/3$ , which implies that a RC-dyad can be synthesized only for  $m = 2$ , or three prescribed poses. This result is well reported in the literature [3,10,11].

The problem at hand is the synthesis with  $m = 3$ , which implies that the number of equations exceeds that of unknowns by one. We have to resort to an approximate method for its solution. The synthesis task is thus formulated as a constrained optimization problem

$$z(\mathbf{x}) = \frac{1}{2} \mathbf{f}^T(\mathbf{x}) \mathbf{f}(\mathbf{x}) \rightarrow \min_{\mathbf{x}} \quad (29)$$

$$\text{s.t. } \mathbf{g}(\mathbf{x}) = \mathbf{0}$$

<sup>4</sup>Angles  $\alpha_j$ , for  $j = 1, 2, 3, 4$ , are associated with a spherical linkage, which does not admit values.

<sup>5</sup>Should the  $j$ th displacement be a pure translation,  $p_j$  would tend to  $\infty$ ; in this case, rather than the pitch, the translation  $d_j$  would be used, as the authors suggested for the planar case [16].

where  $\mathbf{x} = [\mathbf{a}_0^T, \mathbf{b}^T, \mathbf{u}_0^T, \mathbf{v}^T]^T$  and  $\mathbf{f}(\mathbf{x})$  is a six-dimensional vector function of  $\mathbf{x}$ , whose components are

$$\begin{aligned} f_j &= \mathbf{a}_0^T(\mathbf{Q}_j^T - \mathbf{1})\mathbf{b}; \\ f_{j+3} &= \frac{1}{\lambda} \mathbf{a}_0^T \overline{\mathbf{Q}}_j^T \mathbf{b} + \mathbf{a}_0^T(\mathbf{Q}_j^T - \mathbf{1})\mathbf{v} + \mathbf{u}_0^T(\mathbf{Q}_j^T - \mathbf{1})\mathbf{b}, \quad j = 1, 2, 3 \end{aligned} \quad (30)$$

The set of constraint equations  $\mathbf{g}(\mathbf{x}) = \mathbf{0}$  consists of Eq. (9b) for unit constraints and Eqs. (23) and (24) for the vanishing of the sliding, the latter having to be normalized with the characteristic length defined in Sec. 3.2.1.

**3.3.1 Unified Synthesis Equation.** Problem (29) was formulated for RC dyads. It is applicable to CC dyads as well, if we remove the constraints for the vanishing sliding on the fixed axis. Alternatively, we could include additional constraints based on design requirements. For example, in designing a linkage for the closing and the opening of the doors of a fancy sports car, the designer may want to have the axis of the driving joint located at a particular place with respect to the door at the closed location. In this way, the formulation ends up with a set of unified synthesis equations applicable to both RC and CC dyads. While this formulation allows only for an approximate solution for the RC dyad, it leaves room for imposing additional constraints on the CC dyad.

#### 4 Congruences of Fixed and Moving Axes

The synthesis of CC dyads that guide a rigid body through four given poses admits infinitely many solutions. These solutions are sets of lines for the moving and fixed axes, called *congruences*. In the synthesis of planar four-bar linkages with four given poses, circlepoint and centerpoint curves are generated to select pivoting points for moving and fixed-joint centers, respectively. Analogous to the planar case, *congruences* can be defined for the moving and fixed axes of the CC dyads.

Murray and McCarthy [8] developed a parametrization technique for the central-axis congruence of the four-pose rigid-body-guidance problem, utilizing the dual crank angle of rotation as generation parameter. Larochelle [6] developed a procedure to determine the two congruences, whereby the input angle at one joint was discretized to generate the sets of congruences. For each input angle, by assigning the distance between the fixed and the moving axes to two solution lines, Larochelle solved his synthesis equations for two corresponding lines. The two lines were further parameterized to define a plane, i.e., a congruence.

An alternative method of defining and generating line congruences that may be used for fixed and moving axes was proposed in Ref. [10]. The method exploits the three constraint equations, as recalled below.

The direction equations for the four given poses can be rewritten as

$$\mathbf{C}\mathbf{b} = \mathbf{0}, \quad \mathbf{C} = \begin{bmatrix} \mathbf{q}_1^T \\ \mathbf{q}_2^T \\ \mathbf{q}_3^T \end{bmatrix} \quad (31)$$

where  $\mathbf{q}_j$ ,  $j = 1, 2, 3$ , are defined in Eq. (11).

The  $3 \times 3$  matrix  $\mathbf{C}$  must thus be singular, which means that, under the four given poses

$$F(\mathbf{a}_0) \equiv \det(\mathbf{C}) = (\mathbf{q}_1 \times \mathbf{q}_2) \cdot \mathbf{q}_3 = 0 \quad (32)$$

Equation (32) defines a conic surface in Cartesian space. Its intersection with the unit sphere yields a spherical curve, which is called the *spherical circlepoint curve*. Each point on the curve defines a possible unit vector for the moving axis.

Likewise, the equation for the unit vector of the fixed axis has the form

$$\mathbf{G}(\mathbf{b}) \equiv \det(\mathbf{D}) = (\mathbf{p}_1 \times \mathbf{p}_2) \cdot \mathbf{p}_3 = 0 \quad (33)$$

with

$$\mathbf{D} \equiv \begin{bmatrix} \mathbf{p}_1^T \\ \mathbf{p}_2^T \\ \mathbf{p}_3^T \end{bmatrix} \quad (34)$$

The intersection of the cubic surface described by the above equation with the unit sphere yields the *spherical centerpoint curve*. Each point on the latter corresponds to a unit vector for the fixed axis.

Now, as per Eq. (11),  $\mathbf{p}_j$  is linear homogeneous in  $\mathbf{b}$ , while  $\mathbf{q}_j$  is likewise in  $\mathbf{a}_0$ . Consequently, Eq. (32) is cubic homogeneous in  $\mathbf{a}_0$ , while Eq. (33) is cubic homogeneous in  $\mathbf{b}$ . This means that Eq. (32) represents a surface that passes through the center  $O$  of the sphere, i.e., the origin of any of the coordinate frames at hand. Moreover, the line passing through  $O$  in the direction of  $\mathbf{b}$  sweeps a conic surface of apex  $O$ , the counterpart of the *centerpoint curve* in the planar case. Chiang [18] calls this spherical curve the *centerpoint curve*, exactly as in the planar case, with the understanding that this curve is *spherical*.

Likewise, Chiang calls the counterpart intersection of the conic surface swept by the line stemming from  $O$  and directed along the unit vector  $\mathbf{a}_0$  with the unit sphere the *circlepoint curve*. McCarthy and Soh [11] term the foregoing conic surfaces the *center-axis cone* and the *circling-axis cone*, respectively. In this work, we adopt the terminology of *spherical centerpoint and circlepoint curves*, while recognizing their corresponding geometric entities of the spherical cones.

Note that the spherical centerpoint and the circlepoint curves are linked through the direction constraint equation (8a). This means that each point on one of the two curves has its unique image on the other curve.

The dual vector parts of the two axes, i.e., the moments  $\mathbf{a}_0$  and  $\mathbf{b}$ , can be found from Eq. (12). However, for the four-pose case,  $\mathbf{M}$  of Eq. (12) is of  $5 \times 6$ , and the system is underdetermined. The solution proposed in Ref. [10] is to add a sixth row,  $\mathbf{m}_6^T = [1, 0, 0, 0, 0, 0]^T$ , to matrix  $\mathbf{M}$ ; correspondingly, the right-hand side of Eq. (12) becomes  $\mathbf{n} = [w_1, \dots, w_3, 0, 0, \xi]^T$ , which means that the  $x$ -component ( $\bar{\mathbf{a}}_0$ ) <sub>$x$</sub>  of  $\bar{\mathbf{a}}_0$  is assigned a variable value  $\xi$ . If the choice of  $\mathbf{m}_6$  happens to render  $\mathbf{M}$  singular, then another component of  $\bar{\mathbf{a}}_0$  should be chosen instead.

Because of the algebraic coupling between  $\bar{\mathbf{a}}_0$  and  $\bar{\mathbf{b}}$ , the latter also turns out to be a function of parameter  $\xi$ . In this case, Eq. (12) thus yields the moments sought as linear, nonhomogeneous functions of parameter  $\xi$ . We thus obtain solution axes in the form of Plücker coordinates  $[\mathbf{a}_0^T \bar{\mathbf{a}}_0^T(\xi)]^T$  and  $[\mathbf{b}^T \bar{\mathbf{b}}^T(\xi)]^T$ , each standing for a *continuous set* of parallel lines lying in a plane. With this method, the congruences can be generated directly for any given input angle (orientation), without solving again the synthesis equation, which gives computation advantage over other methods.

**4.1 A Robust Formulation of CC-Dyad Synthesis for Four Poses.** In the method recalled above from Ref. [10], the  $x$ -component of  $\bar{\mathbf{a}}_0$  is selected as the parameter in defining congruences. Obviously, this is an element of arbitrariness that can lead to singularities or ill-conditioning, when the  $x$ -component of  $\bar{\mathbf{a}}_0$  is equal or very close to zero. In order to cope with this shortcoming, a robust formulation is proposed below.

The synthesis equation of CC-dyads with four poses ( $m = 3$ ) is formulated as in Sec. 3.1, with the provision that, in that section,  $m$  was 4. We thus still have

$$\mathbf{M}\mathbf{x} = \mathbf{n} \quad (35)$$

but with  $\mathbf{M}$  and  $\mathbf{n}$  of reduced dimensions

$$\mathbf{M} = \begin{bmatrix} \mathbf{p}_1^T & \mathbf{q}_1^T \\ \mathbf{p}_2^T & \mathbf{q}_2^T \\ \mathbf{p}_3^T & \mathbf{q}_3^T \\ \mathbf{a}_0^T & \mathbf{0}^T \\ \mathbf{0}^T & \mathbf{b}^T \end{bmatrix}, \quad \mathbf{x} = \begin{bmatrix} \bar{\mathbf{a}}_0 \\ \bar{\mathbf{b}} \end{bmatrix}, \quad \mathbf{n} = \begin{bmatrix} w_1 \\ w_2 \\ w_3 \\ 0 \\ 0 \end{bmatrix} \quad (36)$$

and

$$w_j = -\mathbf{a}_0^T \bar{\mathbf{Q}}_j^T \mathbf{b}, \quad j = 1, 2, 3 \quad (37)$$

As matrix  $\mathbf{M}$  is of  $5 \times 6$ , the foregoing system of equations is *underdetermined*, and hence, admits infinitely many solutions. The infinity of solutions of Eq. (35) can be represented as

$$\mathbf{x} = \mathbf{M}^\dagger \mathbf{n} + \mathbf{x}_n, \quad \mathbf{M}^\dagger \equiv \mathbf{M}^T (\mathbf{M} \mathbf{M}^T)^{-1} \quad (38)$$

where  $\mathbf{M}^\dagger$  is the *right Moore–Penrose generalized inverse* of  $\mathbf{M}$ , and  $\mathbf{x}_n$  a particular solution that lies in the null space of  $\mathbf{M}$ .

Here, a clarification is in order: generalized inverses have been found in the literature on kinematics, mainly in the realm of screw theory, to lead sometimes to meaningless sums of terms with disparate units. Not in the case at hand. Indeed,  $\mathbf{M}$  is first partitioned row-wise into two blocks

$$\mathbf{M} = \begin{bmatrix} \mathbf{M}_u \\ \mathbf{M}_l \end{bmatrix}, \quad \mathbf{M}_u = \begin{bmatrix} \mathbf{p}_1^T & \mathbf{q}_1^T \\ \mathbf{p}_2^T & \mathbf{q}_2^T \\ \mathbf{p}_3^T & \mathbf{q}_3^T \end{bmatrix}, \quad \mathbf{M}_l = \begin{bmatrix} \mathbf{a}_0^T & \mathbf{0}^T \\ \mathbf{0}^T & \mathbf{b}^T \end{bmatrix} \quad (39)$$

where it is recalled,  $\mathbf{0}$  denotes the three-dimensional zero vector. Therefore,

$$\mathbf{M} \mathbf{M}^T = \begin{bmatrix} \mathbf{M}_u \mathbf{M}_u^T & \mathbf{M}_u \mathbf{M}_l^T \\ \mathbf{M}_l \mathbf{M}_u^T & \mathbf{M}_l \mathbf{M}_l^T \end{bmatrix} = \begin{bmatrix} \mathbf{M}_u \mathbf{M}_u^T & \mathbf{M}_u \mathbf{M}_l^T \\ \mathbf{M}_l \mathbf{M}_u^T & \mathbf{I}_2 \end{bmatrix} \quad (40)$$

with  $\mathbf{I}_2$  denoting the  $2 \times 2$  identity matrix, which occurs in the foregoing lower-diagonal block, because both  $\mathbf{a}_0$  and  $\mathbf{b}$  are unit vectors, as per Eqs. (9a) and (9b). The upper diagonal block has units of length-squared, while the two off-diagonal blocks have units of length. Therefore, although the different blocks bear distinct units, no sums of incompatible terms occur.

The numerical procedure to obtain robustly the solution (38), which should be taken as a formula, and not as a computational means, is derived below

Let the QR-decomposition of  $\mathbf{M}^T$  be [19]

$$\mathbf{M}^T = \mathbf{Q} \mathbf{R}, \quad \mathbf{Q} = [\mathbf{Q}_L \quad \mathbf{q}_r], \quad \mathbf{R} = \begin{bmatrix} \mathbf{U} \\ \mathbf{0}_5^T \end{bmatrix} \quad (41)$$

where  $\mathbf{Q}$  is a  $6 \times 6$  orthogonal matrix—not to be confused with its subscripted counterpart of Eq. (1b), and, even worse, not necessarily proper—while  $\mathbf{R}$  is a  $6 \times 5$  matrix,  $\mathbf{Q}_L$  is of  $6 \times 5$ ,  $\mathbf{q}_r$  is a six-dimensional vector that spans the null space of  $\mathbf{M}^T$  [19],  $\mathbf{U}$  is a  $5 \times 5$  upper-triangular matrix that is nonsingular if  $\mathbf{M}$  is of full rank, and  $\mathbf{0}_5$  is the five-dimensional zero vector. Moreover, the first term of the right-hand side of Eq. (38) can be shown [19] to reduce to

$$\mathbf{M}^\dagger \mathbf{n} = \mathbf{Q}_L \mathbf{U}^{-T} \mathbf{n} \equiv \mathbf{x}_o \quad (42)$$

which is the *minimum-norm solution* of Eq. (35). Vector  $\mathbf{x}_n$ , in turn, can be obtained as a multiple of  $\mathbf{q}_r$ , namely,

$$\mathbf{x}_n = \tau \mathbf{q}_r, \quad \tau \in \mathbb{R} \quad (43)$$

In summary, then, the set of solutions of Eq. (38) can be represented as

$$\mathbf{x} = \mathbf{x}_o + \tau \mathbf{q}_r \quad (44)$$

thereby obtaining a *continuum* of solutions with  $\tau$  as a real parameter.

Further,  $\mathbf{x}_o$  and  $\mathbf{q}_r$  are partitioned into two three-dimensional blocks, the two blocks providing the solutions sought

$$\mathbf{x}_o = \begin{bmatrix} \bar{\mathbf{a}}_o \\ \bar{\mathbf{b}}_o \end{bmatrix}, \quad \mathbf{q}_r = \begin{bmatrix} \mathbf{q}_a \\ \mathbf{q}_b \end{bmatrix} \quad (45)$$

Hence, the continuum of solutions to Eq. (38) can be expressed as

$$\bar{\mathbf{a}}_o(\tau) = \bar{\mathbf{a}}_o + \tau \mathbf{q}_a, \quad \bar{\mathbf{b}}(\tau) = \bar{\mathbf{b}}_o + \tau \mathbf{q}_b, \quad \tau \in \mathbb{R} \quad (46)$$

Therefore, the lines sought,  $Z_2$  and  $(Z_3)_0$ — $Z_3$  at the linkage reference posture—are given by the six-dimensional arrays of Plücker coordinates  $[\mathbf{a}_0^T, \bar{\mathbf{a}}_o^T + \tau \mathbf{q}_a^T]^T$ ,  $[\mathbf{b}^T, \bar{\mathbf{b}}_o^T + \tau \mathbf{q}_b^T]^T$ , respectively. That is, the directions of  $Z_2$  and  $(Z_3)_0$  are given by the infinite set of points on the *spherical centerpoint and circlepoint cubics*, respectively, to each point on one, there corresponds one and only one on the other. Moreover, once the direction of each axis has been chosen from the two curves, their moments, i.e., the location of these two axes, are not unique, but linear, nonhomogeneous functions of the real parameter  $\tau$ . The sets of lines are the *line congruences* sought.

In order to find the location of the points of  $Z_2$  and  $(Z_3)_0$  closest to the origin  $R_0$  of the reference frame depicted in Fig. 1, we resort to the relations used in Ref. [10]. If  $\mathbf{r}_B$  and  $\mathbf{r}_{A0}$  denote, respectively, the position vectors of the foregoing points, then

$$\mathbf{r}_{A0} = \mathbf{a}_0 \times \bar{\mathbf{a}}_o, \quad \mathbf{r}_B = \mathbf{b} \times \bar{\mathbf{b}}_o \quad (47)$$

Now, since  $\bar{\mathbf{a}}_o$  is normal to  $\mathbf{a}_0$  and  $\bar{\mathbf{b}}_o$  is normal to  $\mathbf{b}$ , and both  $\mathbf{a}_0$  and  $\mathbf{b}$  are unit vectors, it is apparent that

$$\|\mathbf{r}_{A0}\| = \|\bar{\mathbf{a}}_o\|, \quad \|\mathbf{r}_B\| = \|\bar{\mathbf{b}}_o\| \quad (48)$$

Therefore, since  $\bar{\mathbf{a}}_o$  and  $\bar{\mathbf{b}}_o$  are both of minimum norm,  $\mathbf{r}_{A0}$  and  $\mathbf{r}_B$  are also of minimum norm.

From the foregoing result, we have that

- given the freedom of choice of  $\mathbf{a}_0$  and  $\mathbf{b}$  in the foregoing problem, CC-dyad synthesis, these two vectors can be used as design variables to minimize some dimensions, which should lead to a compact linkage.
- the line congruences allow for the compliance of additional design requirements, like avoidance of branching defect or the optimization of the transmission angle, once one of the two synthesized dyads has been designated as the input link.

## 5 Examples of Synthesis

We include here examples of spatial linkage synthesis to demonstrate the foregoing method. In the examples, the orientation is described with *natural invariants* [15], i.e., the unit vector  $\mathbf{e}_j$  of the axis of rotation and the angle of rotation  $\varphi_j$ , at the  $j$ th pose. The rotation matrix at this pose then takes the form [15]

**Table 1 Four given poses for Example 1**

No. $\varphi_j$ (rad)	$\mathbf{e}_j^T$	$\mathbf{r}_j^T$ ( $\times 10^{-2}$ )m
1	0	[0, 0, 1]
2	1.3690	[0.1012, 0.6926, -0.7140]
3	1.8602	[0.1542, 0.6014, -0.7838]
4	1.5707	[0.0, 0.3714, -0.9284]

Table 2 Real solutions for a RC dyad of Example 1

	Solution	
$\mathbf{a}_0, \bar{\mathbf{a}}_0$	$[-0.1985, 0.5897, -0.7828],$	$[35.0102, -53.4036, -49.1070] (\times 10^{-2})\text{m}$
$\mathbf{b}, \bar{\mathbf{b}}$	$[-0.0490, -0.7086, 0.7038],$	$[-35.6810, 41.2826, 39.0801] (\times 10^{-2})\text{m}$

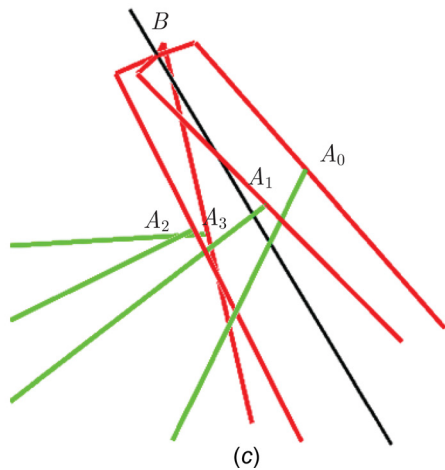
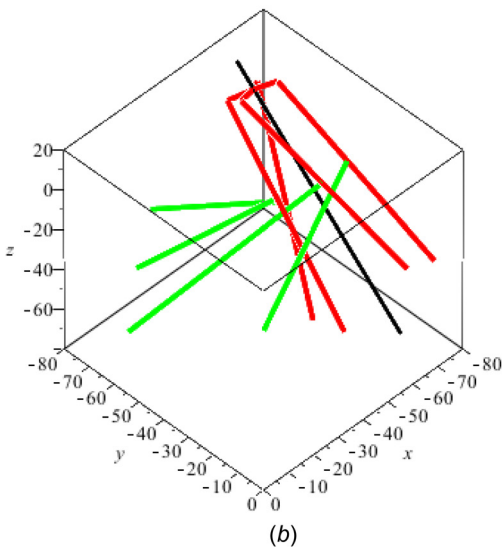
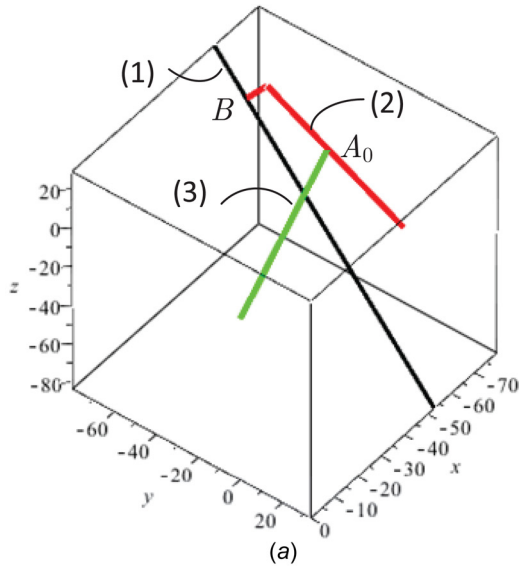


Fig. 5 RC dyad generated from synthesis results: (a) in the reference configuration, where links are numbered with respect to Fig. 1; (b) in all four poses; and (c) zoom-in of the revolute joint

$$\mathbf{Q}_j = \mathbf{1} + \sin \phi_j \mathbf{E}_j + (1 - \cos \phi_j) \mathbf{E}_j^2 \quad (49)$$

where  $\mathbf{E}_j$  denotes the cross-product matrix of  $\mathbf{e}_j$ .

In the synthesis of the RC dyad for four prescribed poses, a system of 11 equations, (8a), (8b), (23), and (24), is obtained. The unknowns at hand include the six components of the two unit vectors and the six components of the two moment vectors. Upon introducing spherical coordinates on the unit sphere, two variables are eliminated

$$\mathbf{a}_0 = \begin{bmatrix} \cos \phi_a \cos \theta_a \\ \cos \phi_a \sin \theta_a \\ \sin \phi_a \end{bmatrix}, \quad \mathbf{b} = \begin{bmatrix} \cos \phi_b \cos \theta_b \\ \cos \phi_b \sin \theta_b \\ \sin \phi_b \end{bmatrix} \quad (50)$$

where  $\theta_a(\theta_b)$  and  $\phi_a(\phi_b)$  are the longitude and the latitude of spherical coordinates. The unit-vector constraints are therefore no longer required, the synthesis problem involving only eight unknowns.

### 5.1 Example 1

**5.1.1 RC-Dyads.** The given poses are displayed in Table 1, where translations carry units of length, as specified. The characteristic length was calculated as  $6.3 \times 10^{-2}$  m, which was used to normalize the “moment” synthesis equations. A set of approximate solutions is obtained from Eq. (29), as listed in Table 2. The synthesis error, namely,  $z(\mathbf{x})$  in this case, is found as a nondimensional  $1.84 \times 10^{-6}$ , which is a good result in approximate synthesis. The results are further examined graphically, as shown in Fig. 5, where links are represented by sticks. A zoom-in of the revolute joint reveals that the vanishing-sliding condition is met by the synthesized linkage.

**5.1.2 CC-Dyad.** For the four given poses of Example 1, the associated spherical centerpoint and circlepoint curves are displayed in Fig. 6, on the unit sphere. Of these, the circlepoint curve is selected to generate the line congruences. Figure 7 shows the congruences of the fixed and moving axes, where long solid edges on each plane indicate the direction of the set of lines. Note that a number of points are selected from the circlepoint curve, as illustrated in Fig. 6(b), to generate the congruences with a clear view. A CC dyad can be selected from the congruences. Alternatively, the dyad can be generated from Eq. (29), which yields an approximate solution.

**5.2 Example 2.** In the second example, the pose data from Ref. [20] are adopted, as listed in Table 3. Using the same approach, a RC dyad is synthesized as listed in Table 4, for which the synthesis error, in terms of  $z(\mathbf{x})$ , is equal to  $1.125 \times 10^{-8}$ . It is noted that the solution is not the same as Ref. [20], which is not surprising, as the objective functions in the two cases are different.

The RC dyads in both examples were synthesized approximately with “small” synthesis errors of  $O(-4)$ . In certain cases, the synthesis may end up with a large error, for which an adjustment of the synthesis task might be needed, for example to adjust the pose of one of the intermediate poses. Notice that  $z(\mathbf{x})$  being one-half the square of the nondimensional approximation error, a value of  $O(-8)$  implies an approximation error of  $O(-4)$ . Finally, the error being nondimensional, its order of magnitude indicates the “size” of the approximation error.

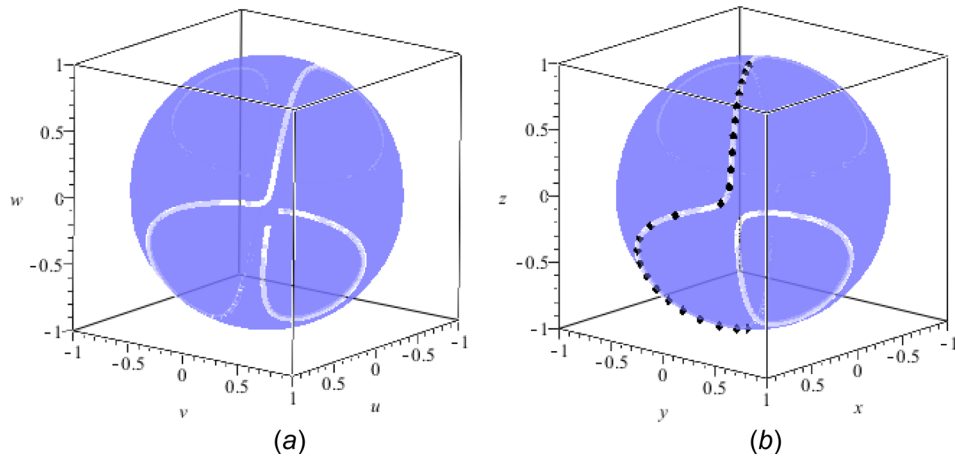


Fig. 6 Cubics on the unit sphere: (a) the spherical centerpoint curve, (b) the spherical circle-point curve

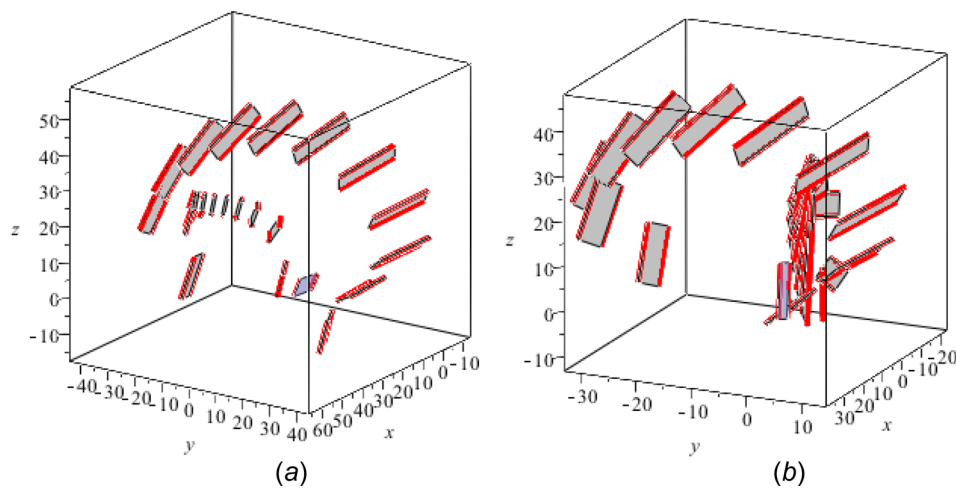


Fig. 7 Congruences of the CC dyad: (a) the fixed axis ( $Z_1$  or  $Z_2$ ) and (b) the moving axis ( $Z_3$  or  $Z_4$ )

Table 3 Four given poses for Example 2

#	$\phi_j$ (rad)	$e_j^T$	$r_j^T$ (m)
1	0	[0,0,1]	[0,0,0]
2	$-0.4 \times 10^{-3}$	[-0.9206, 0.3335, 0.2030]	[-0.0215, 0.0072, 0.0028]
3	3.1189	[0.2349, 0.9268, -0.2931]	[-0.2830, 0.0385, 0.0230]
4	1.7178	[0.8629, 0.3574, 0.3574]	[-0.5000, 0.5000, -2.0000]

Table 4 Real solutions for RC dyad synthesis in Example 2

Solution	
$a_0, \bar{a}_0$	[0.9760, -0.1450, -0.1621] <sup>T</sup> , [-0.3481, -0.4719, -1.6735] <sup>T</sup> (m)
$b, \bar{b}$	[-0.1253, -0.0350, -0.9914] <sup>T</sup> , [-1.8058, -0.1647, 0.2341] <sup>T</sup> (m)

## 6 Conclusions

The spatial Burmester problem was revisited with focus on the synthesis of the RCCC linkage for four prescribed poses. The synthesis equations were derived for spatial RC and CC dyads. The formulation allows the approximate synthesis of the RC-dyad. The formulation is also applicable to CC dyads to yield a feasible solution, when the constraint equations are reformulated, thereby leading to a unified approach for the two cases. This is a first contribution of the paper.

Another contribution lies in the robust formulation of the CC-dyad synthesis equations, from which the congruences to determine fixed and moving axes can be synthesized robustly. Robustness means insensitivity to spurious singularities and ill-conditioning when arbitrarily choosing a given parametrization.

While infinitely many exact solutions to the problem of CC-dyad synthesis exist for the four-pose rigid-body-guidance problem, the RC-dyad synthesis admits only approximate solutions, the RCCC linkage thus being capable of visiting four prescribed poses approximately. In practical applications, additional constraints can be introduced, for example, the volume occupied by the linkage, or visiting one specific pose exactly, as in pick-and-place operations.

## Acknowledgment

The contribution of the second author was possible by the support provided by the James McGill Professorship of Mechanical Engineering and the Velux Visiting Professorship sponsored by The Velux Foundation, Denmark.

## References

- [1] Pérez, A., and McCarthy, J. M., 2003, "Dimensional Synthesis of Bennett Linkages," *ASME J. Mech. Des.*, **125**(1), pp. 98–104.

- [2] Brunthaler, K., Schrocker, H., and Husty, M., 2005, "A New Method for the Synthesis of Bennett Mechanisms," CK2005 International Workshop on Computational Kinematics, Cassino, Italy, May 4–6.
- [3] Tsai, L. W., and Roth, B., 1972, "Design of Dyads With Helical, Cylindrical, Spherical, Revolute and Prismatic Joints," *Mech. Mach. Theory*, 7(1), pp. 85–102.
- [4] Jamalov, R. I., Litvin, F. L., and Roth, B., 1984, "Analysis and Design of RCCC Linkages," *Mech. Mach. Theory*, 19(4–5), pp. 397–407.
- [5] Innocenti, C., 1995, "Polynomial Solution of the Spatial Burmester Problem," *ASME J. Mech. Des.*, 117(1), pp. 64–68.
- [6] Larochelle, P. M., 1995, "On the Design of Spatial 4C Mechanisms for Rigid-Body Guidance Through 4 Positions," ASME Design Engineering Technical Conferences, Boston, MA, Sept. 17–20, pp. 825–832.
- [7] Wampler, C. W., Morgan, A. P., and Sommese, A. J., 1990, "Numerical Continuation Methods for Solving Polynomial Systems Arising in Kinematics," *ASME J. Mech. Des.*, 112(1), pp. 59–68.
- [8] Murray, A., and McCarthy, J. M., 1994, "Five Position Synthesis of Spatial CC Dyads," ASME Mechanisms Conference, Minneapolis, MN, Sept. 11–14, pp. 143–152.
- [9] Huang, C., Kuo, W., and Ravani, B., 2010, "On the Regulus Associated With the General Displacement of a Line and Its Application in Determining Displacement Screws," *ASME J. Mech. Rob.*, 2(4), p. 041013.
- [10] Bai, S., and Angeles, J., 2012, "A Robust Solution of the Spatial Burmester Problem," *ASME J. Mech. Rob.*, 4(3), p. 031003.
- [11] McCarthy, J. M., and Soh, G. S., 2011, *Geometric Design of Linkages*, Springer, New York.
- [12] Martínez, J. R., and Duffy, J., 1993, "The Principle of Transference: History, Statement and Proof," *Mech. Mach. Theory*, 28(1), pp. 165–177.
- [13] Pottmann, H., and Wallner, J., 2001, *Computational Line Geometry*, Springer-Verlag, Berlin.
- [14] Tsai, L. W., and Roth, B., 1973, "Incompletely Specified Displacements: Geometry and Spatial Linkage Synthesis," *ASME J. Manuf. Sci. Eng.*, 95(2), pp. 603–611.
- [15] Angeles, J., 2002, *Fundamentals of Robotic Mechanical Systems*, Springer-Verlag, New York.
- [16] Chen, C., Bai, S., and Angeles, J., 2008, "The Synthesis of Dyads With One Prismatic Joint," *ASME J. Mech. Des.*, 130(3), p. 034501.
- [17] Angeles, J., 2012, "MECH541 Kinematic Synthesis Lecture Notes," Department of Mechanical Engineering, McGill University, Montreal, QC.
- [18] Chiang, C. H., 1988, *Kinematics of Spherical Mechanism*, Cambridge University Press, Cambridge, UK.
- [19] Nash, S., and Sofer, A., 1996, *Linear and Nonlinear Programming*, The McGraw-Hill Companies, Inc., New York.
- [20] Al-Widyan, K., and Angeles, J., 2012, "The Kinematic Synthesis of a Robust RCCC Mechanism for Pick-and-Place Operations," *ASME DETC2012-70878*.